ADVANCED MATERIALS

Supporting Information

for *Adv. Mater.*, DOI: 10.1002/adma.201804416

Near-Infrared Ternary Tandem Solar Cells

*Yongxi Li, Jiu-Dong Lin, Xiao Liu, Yue Qu, Fu-Peng Wu, Feng Liu, Zuo-Quan Jiang, and Stephen R. Forrest**

Supplementary Information

Near-infrared Ternary Tandem Solar Cells

Yongxi Li,[a] Jiu-Dong Lin,[b] Xiao Liu,[a] Yue Qu,[a] Fu-Peng Wu,[b] Feng Liu,[c] Zuo-Quan Jiang,[b] Stephen R. Forrest,[a]*

[a]Department of Electrical Engineering and Computer Science, University of Michigan, Ann Arbor, Michigan 48109, USA.
[b]Institute of Functional Nano & Soft Materials (FUNSOM), Soochow University, Suzhou, Jiangsu 215123, P.R. China.
[c]Department of Physics and Astronomy, and Collaborative Innovation Center of IFSA (CICIFSA), Shanghai Jiaotong University, Shanghai 200240, P. R. China.

[*]*Email: stevefor@umich.edu*

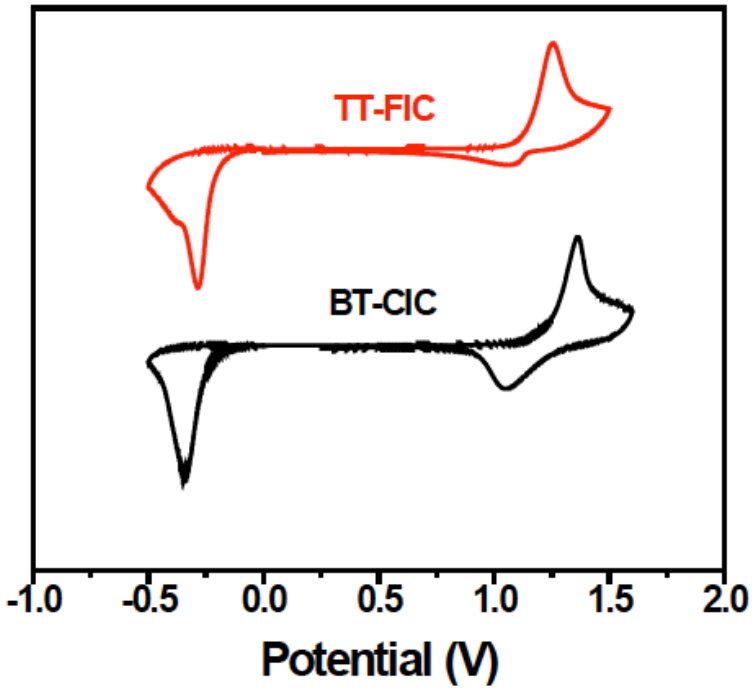

Supplementary Figure 1. Cyclic voltammetry data of BT-CIC and TT-FIC in CH_3CN /0.1 M $[nBu_4N]^+[PF_6]^-$ at 100 mV s^{-1}, the horizontal voltage scale refers to the Ag/AgCl electrode.

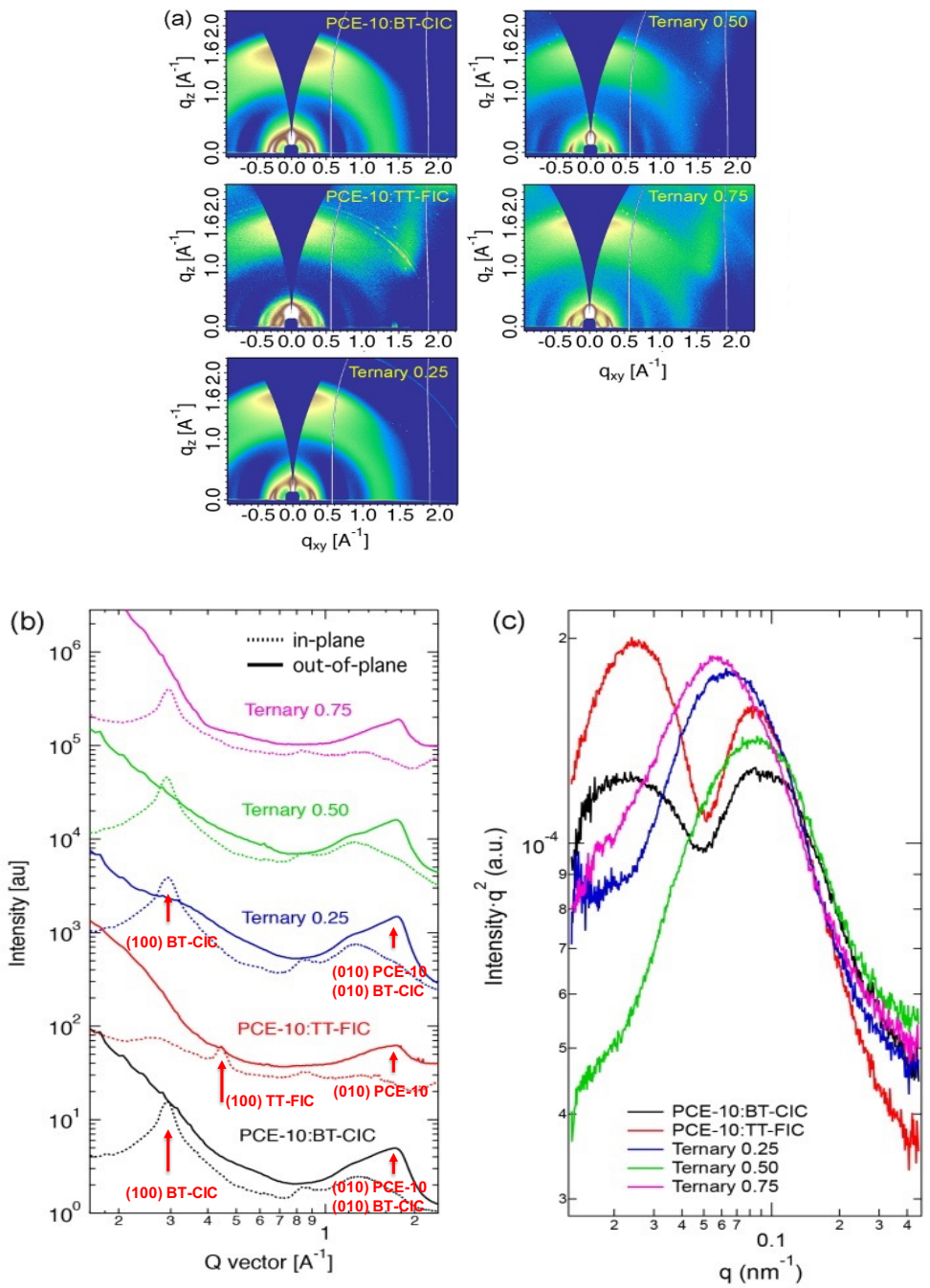

Supplementary Figure 2. (a) 2D glancing incidence x-ray diffraction (GIXD) patterns of binary and ternary blends. (b) In-plane (dotted line) and out-of-plane (solid line) x-ray scattering patterns. (c) Resonant soft x-ray diffraction of binary and ternary blends. *Q* is the scattering vector.

It is seen that the PCE-10:BT-CIC and PCE-10:TT-FIC blends show distinctly different solid state ordering. PCE-10:BT-CIC blends showed stronger diffraction features combined from both PCE-10 and BT-CIC. The crystal coherence length by peak fitting yielded a value of 13.0 nm. In contrast, PCE-10:TT-FIC blends exhibit a weak (100) diffraction peak (0.28 $Å^{-1}$) in the in-plane (IP) direction and the (010) diffraction peak (1.73 $Å^{-1}$) in out-of-plane (OP) direction.

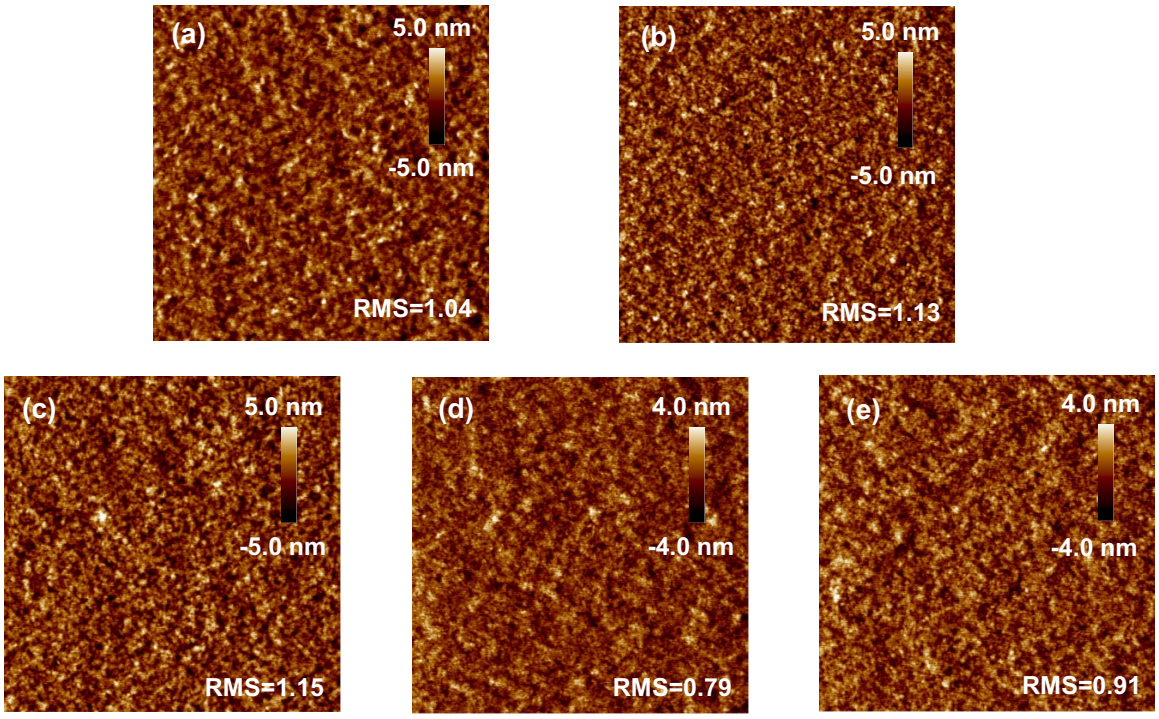

Supplementary Figure 3. AFM topographic image (3 × 3 μm) image of (a) PCE-10: BT-CIC (1:1.5, w/w) and (b) PCE-10:TT-FIC (1:1.5, w/w) and (c) PCE-10: BT-CIC:TT-FIC (1:1.25:0.25, w/w/w) and (d) PCE-10: BT-CIC:TT-FIC (1:1.25:0.5, w/w/w) and (e) PCE-10: BT-CIC:TT-FIC (1:1.25:0.75, w/w/w) blend films cast from 9:1 chlorobenzene:chloroform solution.

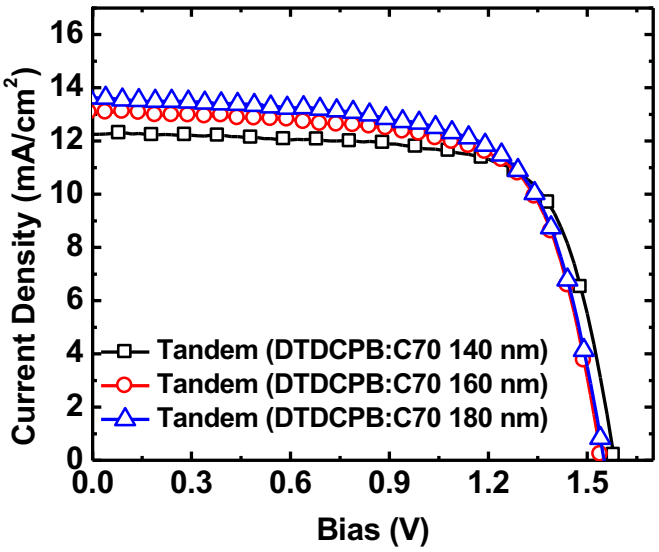

Supplementary Figure 4. Current density-voltage characteristics of tandem cells with various DTDCPB:C_{70} thicknesses.

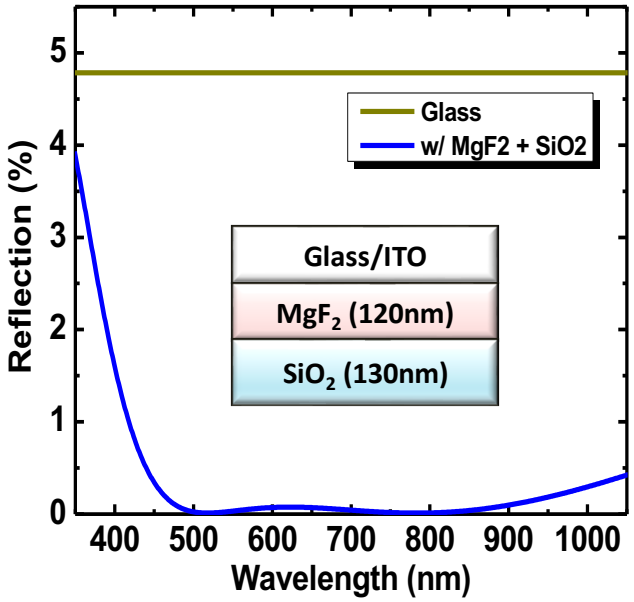

Supplementary Figure 5. Measured reflection ratio between the glass substrates with and without ARC. (Insert: the device architecture of anti-reflection coating.)

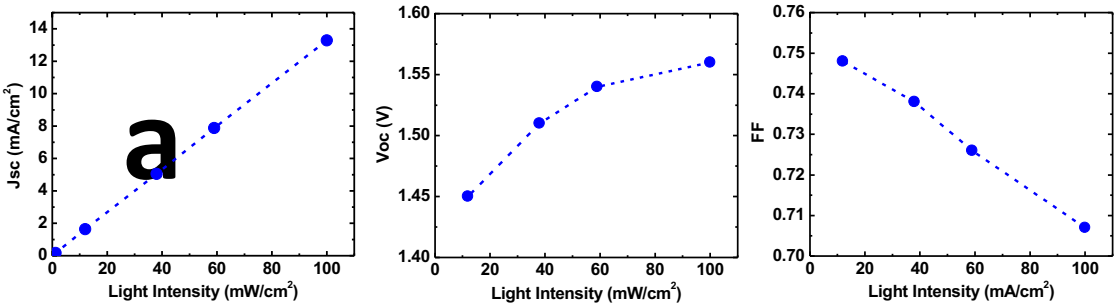

Supplementary Figure 6. J_{SC}, V_{oc} and FF as a function of incident light power density.

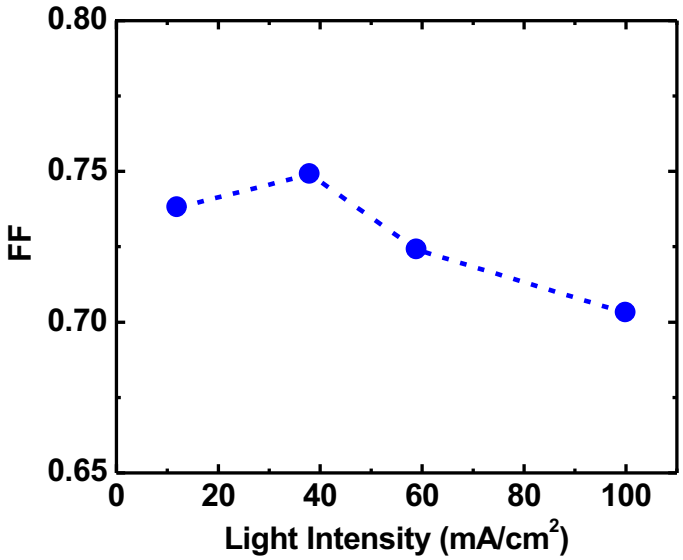

Supplementary Figure 7. The fill factor vs. light intensity for PCE-10:BT-CIC:TT-FIC (1:1.25:0.5, w/w/w) single junction cells.

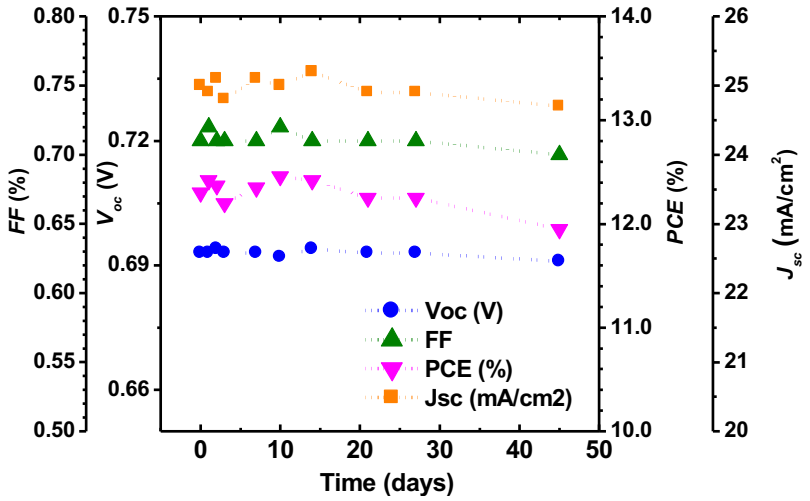

Supplementary Figure 8. Measured ternary device parameters over time. (2 mm^2 device, the devices were kept in the dark between measurements.) Error bars (see Table 1 in the main text) are omitted for clarity.

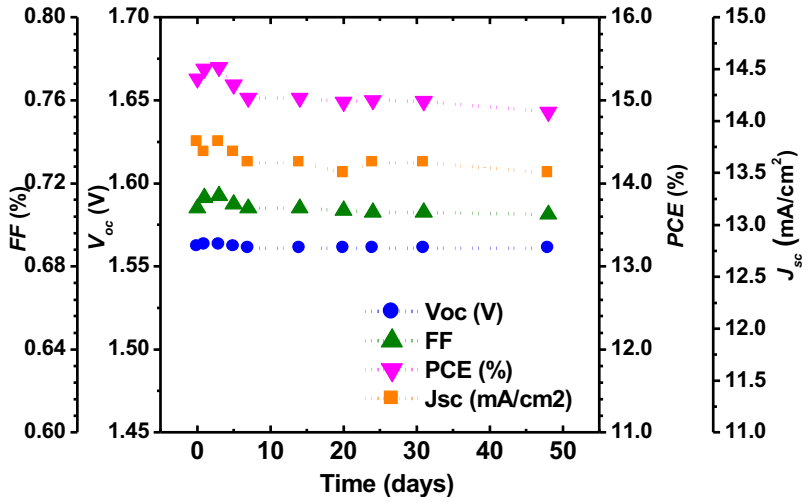

Supplementary Figure 9. Measured tandem device parameters over time (2 mm^2 tandem w ARC, the parameters are measurements of the same cell, the devices were kept in the dark between measurements.). Error bars (see Table 2 in the main text) are omitted for clarity.

Experimental Section

1. *EQE measurement of the tandem solar cell.*

The *EQE* of tandem solar cells were obtained using modulated monochromatic (Thermo Oriel) probe light, which was mechanically chopped at a frequency of 200 Hz. Two LEDs (365 nm, Thorlabs, M365LP1 and 780 nm, Thorlabs, M780L3) are used for bias illumination with wavelengths tuned to excite the photoactive layers in the different subcells. Their intensities are varied with neutral density filters. The three light beams are combined at the tandem cell using lenses, mirrors, and a beam splitter. The sample was encapsulated in the N_2 filled glovebox by sealing a glass lid to the substrate using a bead of UV cured epoxy around its periphery. The packaged cells were maintained in the glovebox during the measurements. The measurements were executed with a lock-in-amplifier over a load of 50 Ω. All data are recorded using LabView. The electrical bias on the tandem cell was provided by the lock-in-amplifier.

The DTDCPB:C_{70} front subcell is insensitive to light at wavelengths longer 780 nm, while PCE-10:BT-CIC:TT-FIC back subcell absorbs up to 1000 nm, as shown in **Figure 5d**,. As a result, bias illumination with a 780 nm light can generate excess charges in the small energy gap back subcell, enabling measurement of the current-limiting wide band gap front subcell in the tandem architecture. On the other hand, the low absorption of the PCE-10:BT-CIC:TT-FIC back subcell in the range of 350 to 500 nm region enables selective optical biasing of the small energy gap back subcell in the *EQE* measurement of

the tandem cell with 365 nm bias illumination. For OPVs where charge collection is often field dependent, the reverse voltage bias that results from optically biased subcells creates additional photocurrent and, hence, an overestimation of the *EQE*[1]. Therefore, an additional forward electrical bias is applied to compensate the reverse bias created on the tandem cell. The electrical bias was determined by making use of *J-V* characteristics of single junction discrete cells under illumination conditions that are representative of the subcells in the tandem.

2. Synthesis Details

Scheme S1. The synthetic routes for TT-FIC.

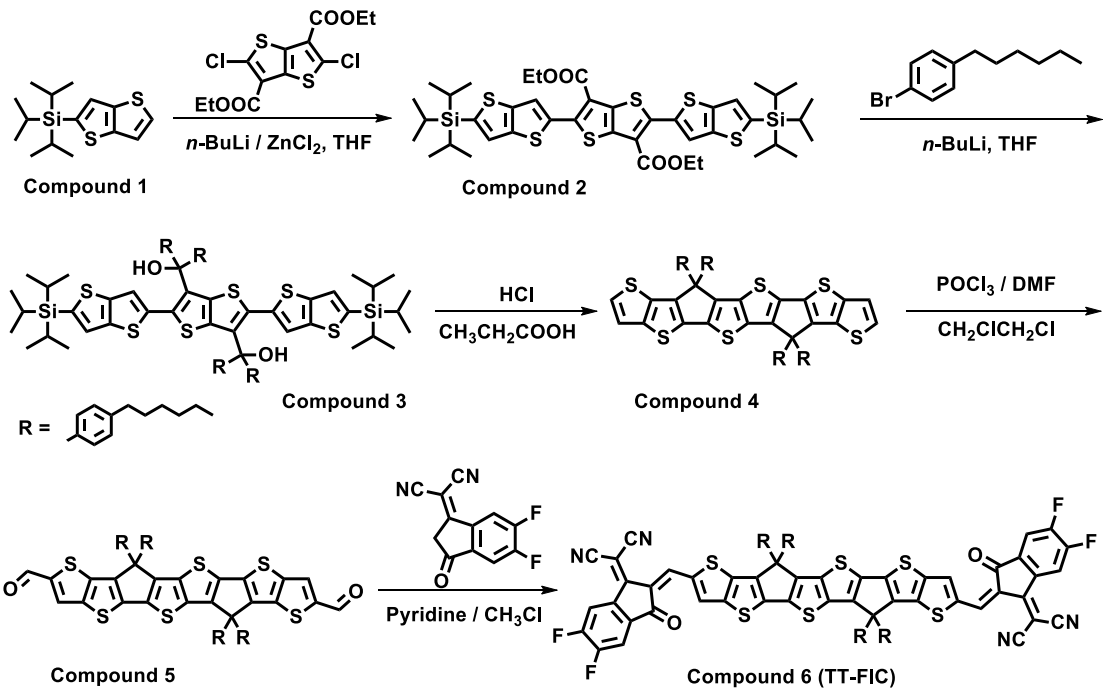

Synthesis of TT-FIC.

3-(dicyanomethylidene)-5,6-difluoro-indan-1-one (207 mg, 0.9 mmol) was added into

the mixture of **Compound 5** (171 mg, 0.15 mmol) in chloroform with pridine (1 mL), the reaction was deoxygenated with nitrogen for 30 min and then reflux for 10 h. After cooling to room temperature, the reaction was poured into methanol and precipitate was filtered off. Then extracted with DCM and washed with water. The crude product was purified by silica gel column using a mixture of hexane/DCM as the eluent to give a purple solid (**Compound 6, TT-FIC**) (189 mg, 81%). ^{1}H NMR (600 MHz, $CDCl_3$, δ): 8.82 (s, 2H), 8.52 (t, J = 12 Hz, 2H), 8.14 (s, 2H), 7.68 (t, J = 12 Hz, 2H), 7.20 (d, J = 12 Hz, 8H), 7.18 (d, J = 12 Hz, 8H), 2.58 (t, J = 12 Hz, 8H), 1.58 (m, 8H), 1.33 – 1.31 (m, 8H), 1.28 – 1.25 (m, 16H), 0.86 (t, J = 6 Hz, 12H). ^{13}C NMR (125 MHz, $CDCl_3$, δ) 185.85, 158.15, 155.27, 153.49, 152.88, 149.96, 148.40, 147.67, 145.81, 143.05, 142.96, 139.75, 138.85, 137.99, 137.95, 137.43, 136.67, 134.43, 129.19, 127.69, 121.09, 114.96, 114.82, 114.38, 114.31, 112.60, 112.47, 69.18, 35.62, 31.67, 31.19, 29.16, 22.57, 14.07.

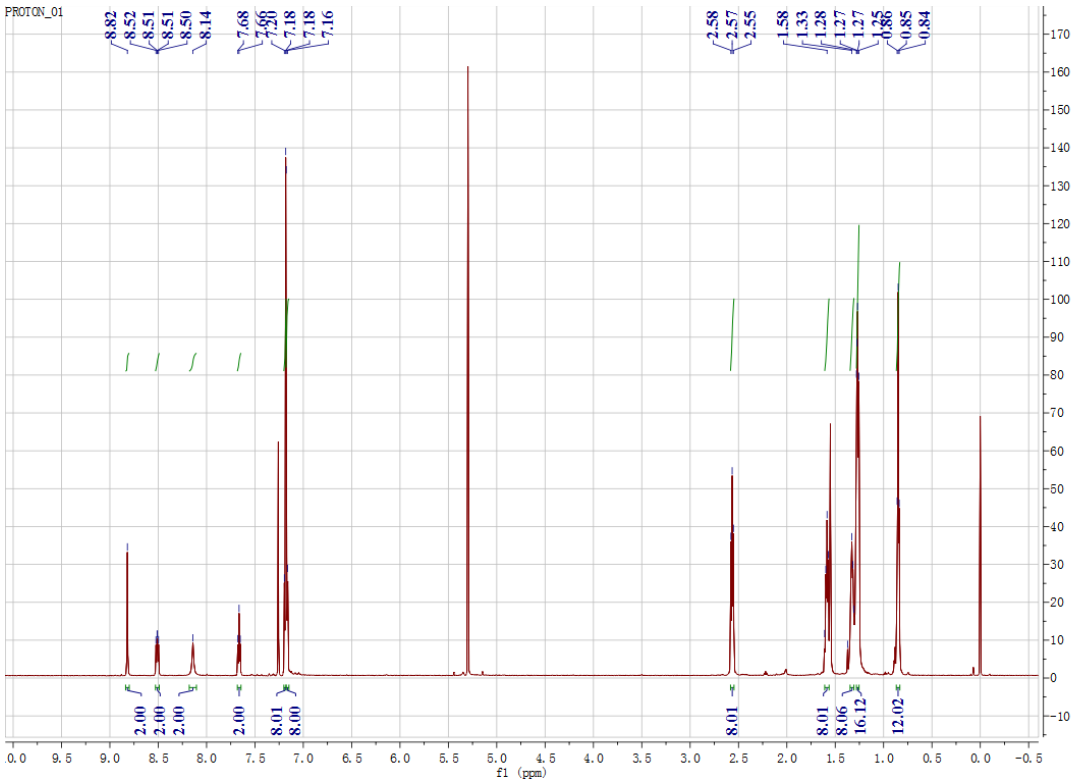

Supplementary Figure 8. ^{1}H NMR of TT-FIC in $CDCl_3$.

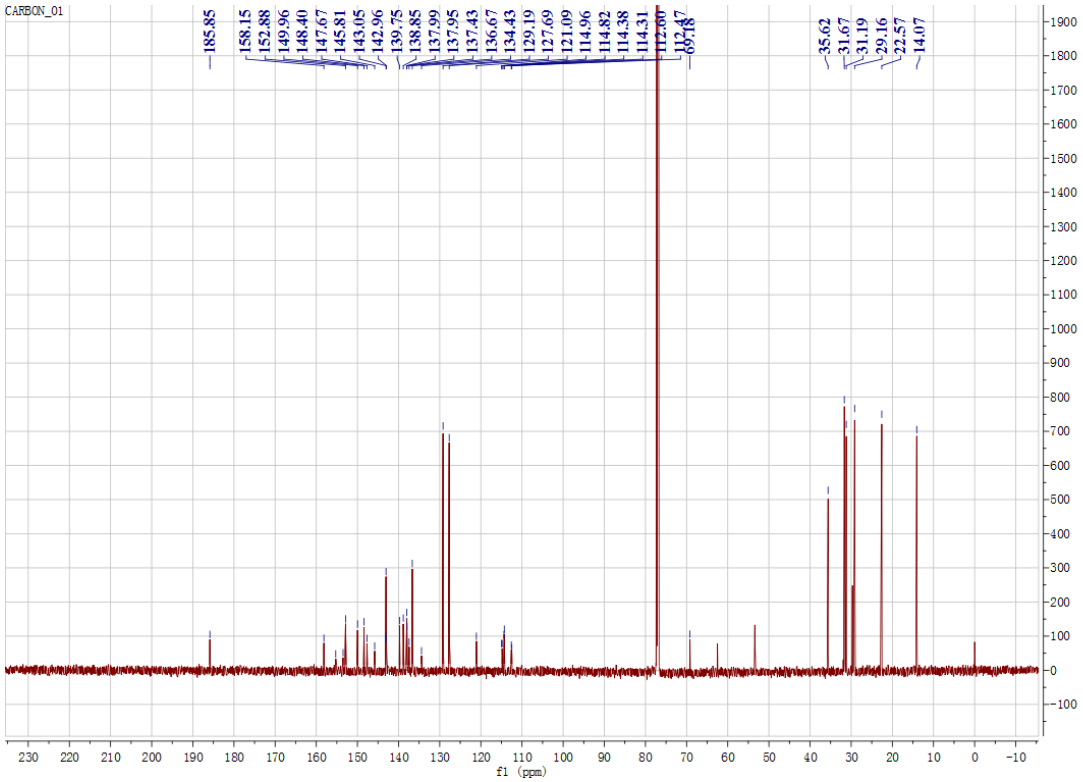

Supplementary Figure 9. *^{13}C* NMR of TT-FIC in $CDCl_3$.

REFERENCES

[1] G. Jan, M. M. Wienk, R. A. J. Janssen, *Adv. Funct. Mater.* **2010**, *20*, 3904-3911.